JOURNAL OF CATALYSIS 87, 255–264 (1984)

Catalytic Gasification of Graphite by Barium in Steam, Carbon Dioxide, Oxygen, and Hydrogen

R. T. K. BAKER, C. R. F. LUND, AND J. J. CHLUDZINSKI, JR.

Corporate Research-Science Laboratories, Exxon Research and Engineering Co.,
Clinton Township, Route 22-E, Annandale, New Jersey 08801

Received June 30, 1983; revised November 18, 1983

Controlled atmosphere electron microscopy studies have demonstrated that barium, derived from $BaNO_2$, is an extremely active catalyst for the graphite–steam reaction at temperatures in excess of 800°C in 2 Torr Ar/H_2O (40 : 1). Continuous observation of the process up to 1150°C shows that the mode of catalytic action is dependent upon the temperature. In the initial stages, particles located at edges and steps on the surface wet and spread along these sites, which then undergo rapid recession. As a consequence, most of the material is utilized during the reaction, making BaO not only a very active additive, but also a very efficient one. As the temperature is raised, there is an increasing tendency for particles to reform at edges, and the catalytic mode changes to channeling. Treatment of the barium/graphite system in carbon dioxide shows parallel behavior to that observed in steam. The oxide is also an active catalyst for the graphite–oxygen reaction, but in this case its activity is similar to that of many other additives. In another series of experiments, barium nitrite/graphite specimens were treated in hydrogen. When barium was activated, it was found to be an effective hydrogenation catalyst for graphite. To achieve this condition, it is necessary to heat the system to 900°C, and then the catalytic channels which are produced will continue to progress even as the temperature is decreased to 700°C. In contrast to the oxidation reactions, the additive did not exhibit any wetting and spreading effects in the hydrogen environment.

INTRODUCTION

Gasification of carbonaceous materials, particularly in a steam environment, is becoming an area of increasing importance in a number of commercial processes. Unfortunately, this process is quite slow and one is therefore forced to look at the possibility of introducing catalysts to increase the rate of gasification.

Studies by previous workers (*1–4*) have shown that barium is one of the most active catalysts for the graphite-steam reaction. Everett *et al.* (*1*) reported that the addition of 0.05% barium increased the rate of reactivity of graphite powder towards water vapor at 850°C by a factor of 10^3. McKee (*2*) used thermogravimetric techniques to examine the effect of several alkaline earth carbonates, including barium carbonate, on the graphite–steam reaction and was able to gain some insight into the possible mechanism of the catalytic reaction. He postulated that the following oxidation–reduction cycle was involved in the $BaCO_3$ catalyzed graphite–steam reaction:

$$BaCO_3 + C \rightarrow BaO + 2CO \qquad (1)$$

$$BaO + H_2O \rightarrow Ba(OH)_2 \qquad (2)$$

$$Ba(OH)_2 + CO \rightarrow BaCO_3 + H_2 \qquad (3)$$

giving the overall reaction:

$$C + H_2O \rightarrow H_2 + CO \qquad (4)$$

Further support for this proposed series of reaction steps was recently obtained by McKee and Yates (*3*), who used a combination of thermogravimetry, mass spectrometry, and selective isotopic labeling to study the steam gasification of graphite in the presence of $Ba^{13}CO_3$. In this reaction sequence, reaction (1) was suggested as the probable rate determining step, the activa-

0021-9517/84 $3.00

tion energy for which was found to be in the range of 40.2 to 46.9 kcal mole^{-1}.

Otto and Shelef (*4, 5*) compared the catalytic influence of several elements on the steam gasification of graphite and concluded that there was a major difference in the mode of catalyst action between the alkaline earths and the Group VIII noble transition metals. Their understanding was that the alkaline earths have the ability to increase the reaction-site density of the carbon by maintaining contact with the surface throughout the reaction. They rationalized the relatively high activity of barium compared to other alkaline earth additives as being due to the fact that barium produced an even coverage on the carbon surface and was therefore successful in converting each surface carbon atom into a reaction site. In contrast, they argued that the noble metals have a tendency to coalesce into large particles and during the gasification reaction become isolated from the graphite surface.

There are, surprisingly, very few reports in the literature pertaining to work on the catalytic effect of barium on graphite gasification in other gaseous environments. Heintz and Parker (*6*) analyzed data obtained by Amariglio (*7*) and reported a value of $\sim$10 kcal mole^{-1} for the activation energy of the barium catalyzed graphite-oxygen reaction.

In the present investigation we have used controlled atmosphere electron microscopy to follow the changes in catalyst particle morphology accompanying the barium catalyzed gasification of graphite in steam, carbon dioxide, oxygen, and hydrogen. It was hoped that this type of experimental approach might provide a clearer understanding of the manner by which barium functions as a catalyst in these systems.

EXPERIMENTAL

All the work described in this paper was performed in the controlled atmosphere electron microscope (*8*). Temperatures reported here are those of the graphite support, measured by means of a Pt/Pt 13% Rh thermocouple spot welded to a platinum heater strip at a point close to the position of the specimen. It is possible that the actual temperature of catalyst particles may differ from that of the support due to endothermic or exothermic processes taking place at their surfaces. For this reason kinetic parameters, such as activation energies are quoted in apparent rather than absolute terms. Barium was applied to single-crystal graphite transmission specimens as an atomized spray from a 0.1% aqueous solution of barium nitrite, which thermally decomposed to form barium oxide (BaO) at 217°C.

The reactant gases used in this investigation, carbon dioxide, oxygen, argon, and hydrogen, were obtained from Scientific Gas Products, Inc. with stated purities of 99.999%. All gases were used without further purification. Experiments where the effects of steam were being studied were performed by allowing the carrier gas to flow through a bubbler containing deionized water maintained at 25°C; this procedure produced a gas/water ratio of about 40/1.

RESULTS

Barium/Graphite—Steam

When graphite specimens containing the atomized barium nitrite were heated in 2 Torr argon saturated with water at 25°C, nucleation of small particles was observed to take place over the temperature range, 300 to 400°C. At 450°C particles had grown to 10 to 20 nm in size and those located along the graphite edges and steps were in a nonwetting condition, i.e., they exhibited contact angles with the surface of >90°. As the temperature was increased, the morphology of these particles underwent a dramatic change. At 500°C the particles rearranged to a condition where wetting of the graphite occurred, i.e., the contact angle decreased to <90°. This situation persisted until about 600°C when particles started to disappear due to further wetting and spreading of material to form a film along the edge sites.

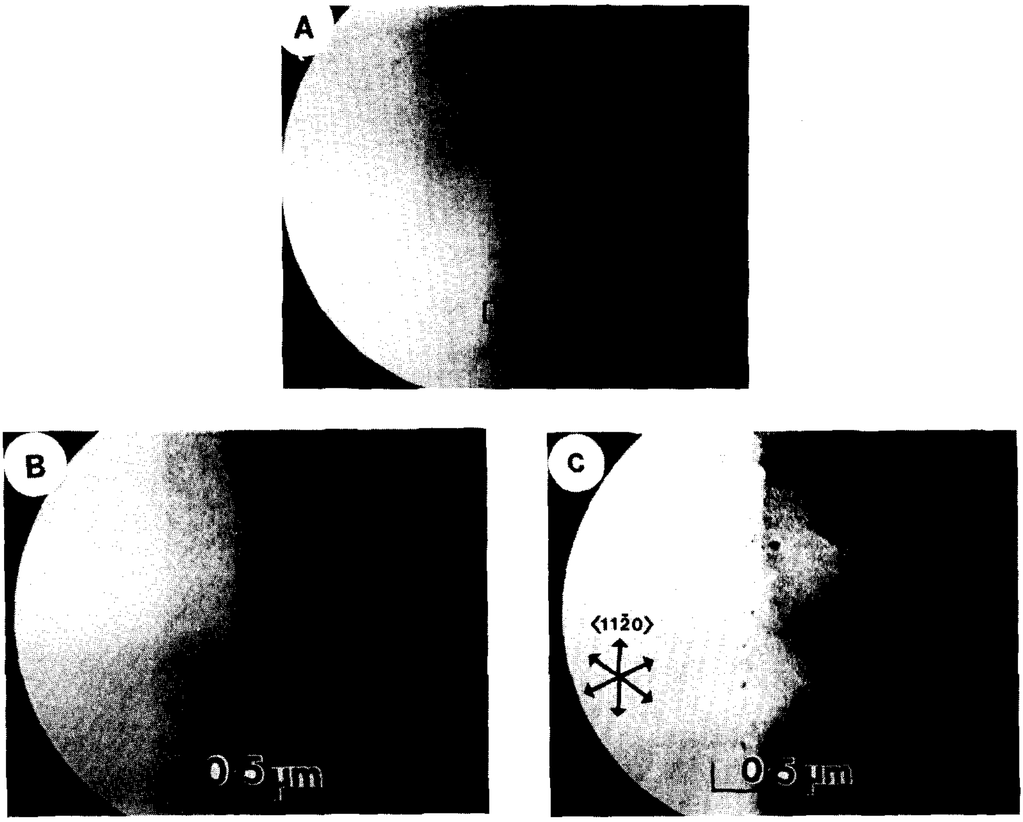

FIG. 1. (A, B) Sequence showing the disappearance of barium oxide particles as they spread along the graphite edges at 600°C in 2 Torr wet argon. (C) Barium oxide catalyzed edge recession of graphite in 2 Torr wet argon at 700°C.

Figures 1A and B are stills taken from the video playback showing this phenomenon. On continued heating, edges and steps were observed to recede in a very uniform manner and along directions parallel to $\langle 11\bar{2}0\rangle$ orientations (Fig. 1C).

Throughout this period particles located on the more perfect basal plane regions of the graphite continued to grow, reaching an average size of 35 nm at 710°C. As the temperature approached 790°C, the majority of particles became mobile on the surface and this resulted in an increase in the number of particles becoming located at edges. The subsequent behavior of such particles was extremely dependent upon the nature of edges with which they came into contact. Previously inactive particles which collided with edges appeared to "dissolve" in them. Immediately afterward, these edges proceeded to undergo rapid recession. When the interaction occurred with edges which were already in the process of undergoing recession, then these particles proceeded to create channels across the graphite surface in the manner depicted schematically in Fig. 2. The catalyst particles were diminished in size as material was left as a film on the channel walls due to the wetting and spreading action. As a consequence, the width of the channels was progressively reduced and edges receded at a rapid rate causing channels to acquire a fluted appearance. Eventually when all material from a given catalyst particle had been depleted, forward progression of that particular channel ceased. Kinetic analysis of several edge recession sequences has enabled an Arrhe-

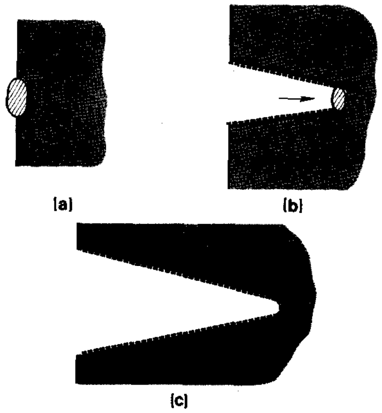

FIG. 2. Influence of wetting and spreading effects on the catalytic channeling mode.

nius plot to be constructed of this data (Fig. 3) and from the least-squares slope of the line an apparent activation energy of 49.1 ± 5 kcal $mole^{-1}$ has been calculated.

A subtle change in the mode of catalytic action was detected at about 900°C; edge recession was no longer uniform tending instead to take on a more ragged outline, and there was evidence that many more particles were creating channels. This transformation in behavior became more pronounced at higher temperatures, >1000°C, as edge recession appeared to decrease in rate and channels followed straight paths, occasionally altering course by bending through angles of 60 and 120° and maintaining definite orientations parallel to $\langle 11\bar{2}0\rangle$ directions. It was also interesting to find that under these conditions the width of channels remained constant for relatively long periods of time. This whole sequence of events is depicted schematically in Fig. 4. When the temperature was reduced to 750°C, the original edge recession activity was restored as particles located at edges and channels tips were observed to wet and spread on the graphite.

If the reaction was performed in an argon stream containing equal amounts of water and hydrogen, then not only was the rate of reaction decreased but also there was a marked reduction in the degree of spreading-edge recession and a corresponding increase in channeling action. Furthermore, on cooling down from the high temperature channeling regime, there was no return to the spread state, instead channel activity continued down to 650°C.

The variation in rate of channel propagation in 2 Torr argon/steam was determined as a function of temperature. To allow for the effect of particle size and channel depth on rate, these measurements were made on

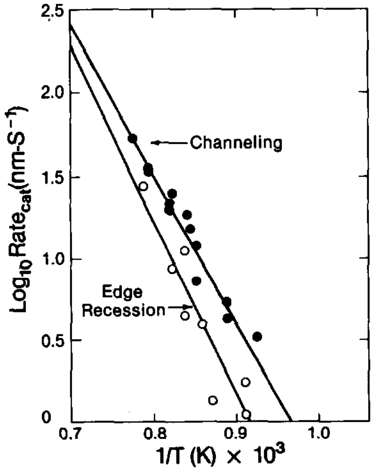

FIG. 3. Arrhenius plot of barium oxide catalyzed gasification of graphite in steam; ●, channeling mode, ○, edge recession mode.

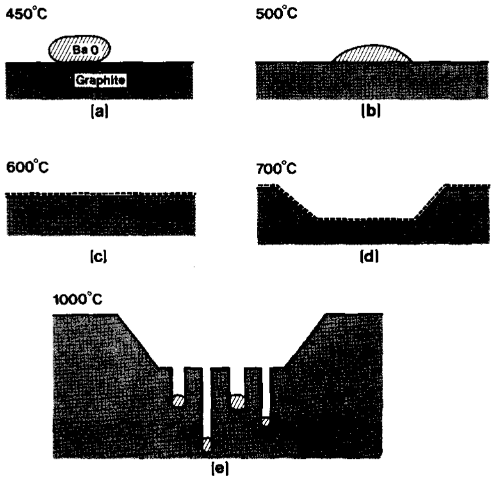

FIG. 4. Behavioral pattern of barium oxide particles on graphite in steam.

particles of constant size, 30 nm, creating channels of similar depth. When these data are presented in the form of an Arrhenius plot (Fig. 3), it is possible to evaluate an apparent activation energy of 43.4 ± 4 kcal mole^{-1} for the barium catalyzed steam gasification of graphite. This figure is in excellent agreement with the values obtained from bulk experiments by McKee of 40.2 (*2*) and 46.9 kcal mole^{-1} (*3*).

Barium/Graphite—Carbon Dioxide

Treatment of the barium/graphite system in CO_2 showed parallel behavior to that found in the presence of steam. Discrete particles were observed to nucleate from the applied barium nitrite solution when the samples were heated to 510°C in 2 Torr CO_2. As the temperature was increased particles located along edges and steps on the basal planes of the graphite progressed from a nonwetting to a wetting condition and then, at 690°C, to a spread state. In this spread state, the barium was capable of catalyzing the gasification of graphite. This process was seen as the uniform recession of edges along which the catalyst had previously dispersed. The rate of edge recession was so slow that it was only apparent by the use of time-lapse photography. Rates of edge recession measured over the range 740 to 895°C are presented in Fig. 5 in the form of an Arrhenius plot from which an apparent activation energy of 32.5 ± 4 kcal mole^{-1} was determined.

A moderation in edge recession activity was observed at 840°C as particles started to reform along the edges and, at 895°C, most catalytic activity was due to channel propagation. Unfortunately, the kinetics of the channeling action were neither reproducible nor consistent. For example, within the same field of view, it was often possible to observe two particles of the same size channeling at the same apparent depth but exhibiting significantly different rates. Channels exhibited no preferred orientation with respect to the graphite crystallographic directions and tended to follow random pathways.

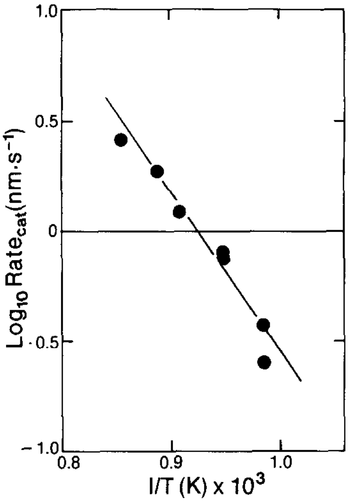

FIG. 5. Arrhenius plot of barium oxide catalyzed edge recession in carbon dioxide.

Barium/Graphite—Oxygen

When the barium/graphite system was exposed to 5 Torr oxygen, the evaporated film of barium nitrite collected up into discrete particles (5 to 15 nm diameter) at 420°C. The first signs of catalytic attack on the graphite were observed at 520°C, taking the form of irregular erosion of edges with the occasional formation of short channels. Attack by the channeling mode became more prolific as the temperature was raised to 575°C, but at this stage edge recession was variable and did not appear to follow any particular orientation. This reactivity pattern was maintained up to 750°C and as temperature was increased so the number and limiting size of particles which displayed catalytic action also increased. During this period the channel characteristics remained unchanged, tending to follow a random path and remain parallel-sided for relatively long periods of time.

Above 750°C, a dramatic change in the nature of the channels was evident, which was similar in behavior to that presented in schematic form in Fig. 2. Active catalyst particles were observed to shrink as material was deposited on the channel walls due to a wetting and spreading action. As a consequence, the width of the initially formed channel decreased and channel walls receded at a faster rate than uncontaminated edges or steps, causing the channels to acquire a fluted appearance. It was also apparent that many particles which came into contact with edges or steps underwent rapid reorganization, spreading along these features as a thin film in preference to remaining as discrete particles and producing channels. Immediately following this behavior, the coated edges and steps proceeded to gasify in a very orderly manner creating the saw-toothed appearance shown in Fig. 6. Detailed examination of the orientation of these regions revealed that edge recession occurred along directions parallel to $\langle 10\bar{1}0 \rangle$ crystal planes.

The reaction was continued up to 950°C when edge recession was the only form of attack, being a combination of catalyzed and uncatalyzed reactions. At this stage very little material appeared to remain on the graphite surface. Mobility of previously inactive particles occurred at 805 to 840°C, and this resulted in most of the barium becoming located at the graphite edge sites and transforming into the film arrangement via the spreading phenomenon.

Quantitative kinetic analysis was performed on the rate of formation of channels as a function of temperature. Because of the spreading behavior of the catalyst particles, it was difficult to obtain meaningful data, and as a compromise the initial size and rate of channel propagation was used. The results obtained for 30-nm-diameter particles are presented in the form of an Arrhenius plot (Fig. 7) and the apparent activation energy derived from this relationship is 12.0 ± 2 kcal mole^{-1}. In view of the problems associated with the analysis of these experiments, we believe that this figure may be subject to considerable error.

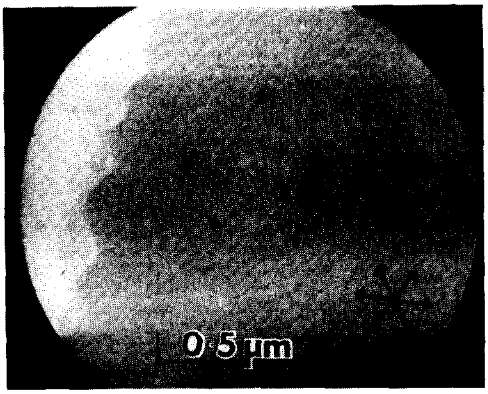

FIG. 6. Barium oxide catalyzed edge recession of graphite in 5 Torr oxygen at 800°C.

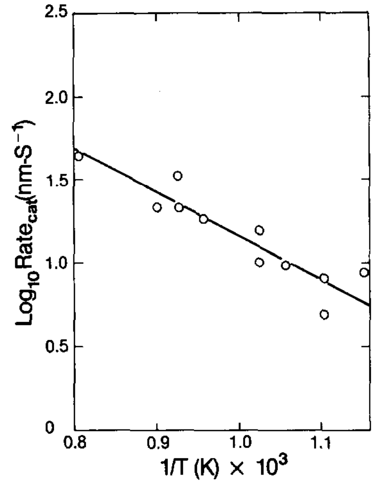

FIG. 7. Arrhenius plot of barium oxide catalyzed gasification of graphite in oxygen.

Barium/Graphite—Hydrogen

Nucleation of the barium film into discrete particles was extremely sluggish when specimens were treated in 1.0 Torr hydrogen, a temperature of 525°C being required to complete the process. With the exception of an increase in average particle size and the finding that some of the particles exhibited temporary mobility at 676°C, no further change in the appearance of the surface occurred until 935°C. At this temperature, particles located on edges started to catalytically attack the graphite by the channeling mode. As the channels developed, it was evident that they possessed all the characteristics normally associated with catalytic hydrogenation of graphite (*9*). The tracks were extremely straight and when they changed direction they did so by bending through 60 and 120° angles. The majority of channels tended to be oriented parallel to the $\langle 11\bar{2}0\rangle$ crystallographic directions.

The reaction was continued up to a maximum temperature of 1050°C, a condition where the rate of reaction was quite rapid, but the channels still remained parallel-sided throughout their propagation period indicating that the rate of uncatalyzed attack was insignificant. Although splitting of active particles was a common event, the catalyst did not have the tendency to exhibit the spreading action seen with nickel under similar experimental conditions (*10, 11*).

It was interesting to discover that if the temperature was gradually reduced, then the channeling activity persisted down to 670°C. Furthermore, on subsequent temperature cycling between 670 and 1050°C, reproducible behavior was obtained. In contrast to the reactions of barium/graphite with steam and oxygen, where edge recession accounted for a large fraction of the overall gasification rate, in this case channel propagation was the sole form of attack.

Quantitative kinetic analysis of channeling sequences showed that at any given temperature, the larger catalyst particles generated channels at the fastest rates for channels of similar depth. It was also possible to derive an apparent activation energy of 33.8 ± 4 kcal mole^{-1} for the barium-catalyzed hydrogenation of graphite (Fig. 8). To compensate for the effects of particle size and channel depth on rate, these measurements were obtained from 25-nm-diameter particles cutting channels of similar depth, and in many instances the same particle was followed at several different temperatures.

DISCUSSION

Several important aspects have emerged from this study, the most notable being the discovery of the ability of barium oxide to wet and spread along graphite edges and steps in both steam and oxygen. Undoubtedly, it is this property which results in barium oxide being a very efficient graphite oxidation catalyst by maximizing the area of contact between available barium atoms and potentially active carbon sites. This is a direct verification of the postulate made by Otto and Shelef (*5*) based upon bulk kinetics. However, in contradistinction, not all carbon atoms were observed to be activated, but only those located at edges.

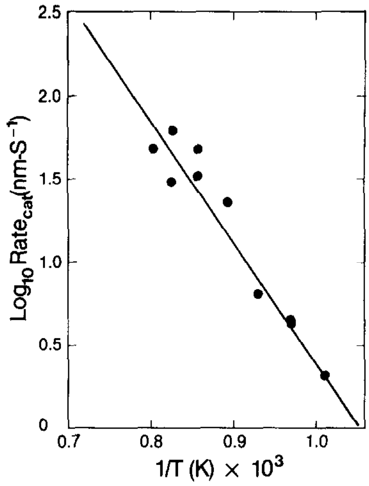

FIG. 8. Arrhenius plot of barium catalyzed hydrogenation of graphite.

For a particle to wet and spread on a support, certain thermodynamic and kinetic criteria must be satisfied. At any point of contact between phases, equilibrium of interfacial energies can be represented by a force diagram for surface tension (*13*) and related to one another according to Young's equation:

$$\sigma_{sg} = \sigma_{ms} + \sigma_{mg} \cos \theta \qquad (5)$$

where σ_{sg} (support–gas), σ_{ms} (metal–support), and σ_{mg} (metal–gas) are the three characteristic surface (interfacial) tensions, and θ is the contact angle between the metal particle and the support. For values of θ <90°, wetting of the support by metal will occur and in the extreme that θ approaches 0° then the particle will tend to spread and cover the support in the form of a thin film. Factors which promote the attainment of this condition are those which result in high values for σ_{sg} and low values for both σ_{ms} and σ_{mg}.

In the present case, the surface tension of barium oxide (σ_{mg}) is quite low, being 290 erg cm^{-2} at 1000°C (*14*). In a previous study (*15*) we estimated a value for the surface tension of the C-faces of graphite to be of about 4500 erg cm^{-2} at 965°C. Chemisorption of either water vapor or oxygen onto the graphite edges will result in a reduction in the value of σ_{sg}, however, this figure will still be very large. No data are available for σ_{ms}, the surface tension between barium oxide and graphite. Despite this lack of information, we believe that the thermodynamic conditions favor a strong interaction between barium oxide and graphite, and, provided that atomic mobility exists in the particles, then wetting and spreading is likely to take place.

Although edge recession is the major mode by which barium oxide catalyzes graphite gasification in both steam and oxygen, there is a distinct difference in the behavior of the two systems. In the presence of oxygen, attack occurs parallel to the $\langle 10\bar{1}0 \rangle$ directions, whereas in steam, recession takes place parallel to the $\langle 11\bar{2}0 \rangle$ crystal planes. This difference in orientation may arise from a tendency of oxygen and steam to chemisorb at particular carbon sites. Indeed, Magne and Duval (*16*) have demonstrated that steam preferentially chemisorbs at $\langle 10\bar{1}0 \rangle$ sites and as a consequence during gasification would selectively remove these carbon atoms leaving behind those in a $\langle 11\bar{2}0 \rangle$ configuration.

Another distinction between the steam and oxygen cases is the order of events: in oxygen, the catalyst channels initially and gradually switches over to an edge recession mode which it maintains to the highest temperatures studied—in steam the inverse occurs. This can be related, at least partially, to the oxidizing/reducing potential of the gas phase and to the concentration of adsorbed oxygen on edges and steps. For example, as the temperature is increased, the discrete particles will start to become partially reduced by the carbon. If the gas phase is not capable of reoxidizing this region of the particle, either because it is not in contact with the gas phase or because some step in the reoxidation process (e.g., dissociation) is too slow, the particle may seek other sources of oxygen. One such source of oxygen is the adsorbed oxygen located along edges and steps. Using this rationale, the reoxidation step in an O_2 atmosphere must be sufficiently rapid at lower temperatures, but as the temperature is increased it must become inadequate, and, hence, spreading and edge recession occur. In contrast, the reoxidation by H_2O must always be slow compared to reduction, and, hence, spreading and edge recession are observed from the outset. However, in the present apparatus, as the temperature increases the product H_2 may build up through residence time effects. Hence, the H_2O/H_2 ratio decreases and less oxygen will be adsorbed on the edges and steps. Eventually the depletion of the adsorbed oxygen will become severe enough to result in renucleation of particles. While at present this explanation is largely postulation, it is supported by the finding that the extent of edge recession was reduced when hydrogen was added to the argon/steam reactant gas. In agreement with previous work (*17*), it was found that this procedure also resulted in a decrease in the rate of the graphite–steam reaction.

From the quantitative data it is possible to obtain a rough estimate of the relative contributions of the two modes of catalytic attack toward the overall steam gasification rate. The number of moles of carbon gasified per second, dn/dt, is given by

$$\frac{dn}{dt} = \frac{2lD\delta\rho}{M}$$

where l is the rate of channel propagation or edge recession (nm s^{-1}), D is the width of channel or receding edge (nm), δ is the depth of the channel or edge (nm), ρ the density of graphite (2.25×10^{-21} g nm^{-3}), and M the atomic weight of carbon. At 825°C, 30-nm-diameter particles create channels at a linear propagation rate of 3.30 nm s^{-1}. If one assumes that the depth of the channel is 10 nm, then the number of moles of carbon gasified per second by this particle is 1.86×10^{-19}. Under these conditions, the particle would typically move a distance of 750 nm before complete dissipation as a thin film along the channel walls. At 825°C, the amount of carbon gasified per second by a receding edge of total length, 1500 nm and thickness 10 nm, moving at a rate of 1.11 nm s^{-1} is 3.09×10^{-18} mol s^{-1}. It is therefore apparent that edge recession is the more important mode of catalytic attack in the barium/graphite–steam reaction.

It is interesting to compare the catalytic pattern of barium on the graphite-oxygen reaction found here with that reported by Cairns and co-workers (*18*) for calcium on the same reaction. They observed that the catalytic particles produced pits on the basal plane regions of the graphite. This type of attack normally occurs at vacancies or screw dislocations in the graphite surface (*19*). The failure to find evidence of pitting in the present study may not necessarily reflect a major difference in the behavior of barium compared to calcium but merely be a result of the relative perfection of the graphite crystals used in two studies.

It is also clear that the strong interaction between barium oxide and graphite is only maintained in a net oxidizing environment; reaction in hydrogen resulted in the barium assuming a particulate rather than thin film morphology. From the sequence of events surrounding the influence of barium on the graphite–hydrogen reaction, it is apparent that after an initial high temperature excursion to obtain the active catalyst that barium is a very active catalyst for this reaction. It is intriguing to compare the morphological behavior of barium with nickel in the graphite oxidation and hydrogenation reactions (*10, 11*). In contrast to barium, nickel remains as discrete particles under oxidizing conditions and tends to spread along graphite edges when heated in hydrogen to temperatures in excess of 1000°C. This mismatch can only be understood from a consideration of all the factors embodied in Young's equation and highlights the need to be aware of the magnitude of these parameters before predicting the probability of whether a given system will exhibit wetting or nonwetting behavior.

The results of carbon dioxide gasification are not understood at present. We believe that it is likely that in this system the electron beam is affecting the reaction. In this context, it is interesting to find that Keep and co-workers (*18*) also experienced difficulties in reproducibility of rate measurements in their CAEM studies with nickel/graphite in carbon dioxide. (Note also that considering the reactant partial pressures, the relative edge recession rates in CO_2 and H_2O are markedly different, whereas bulk measurements show the net rates to be comparable (*2, 19*).

CONCLUSIONS

The efficiency of barium as a steam and oxygen gasification catalyst has been demonstrated to be at least partially due to the catalyst's ability to maintain high dispersion. A model has been proposed to explain this phenomenon. In steam gasification, the produced hydrogen has been shown to cause inhibition of the reaction rate directly and through reducing the tendency for barium to remain highly dispersed. In contrast, the catalyst dispersion is lower during hydrogen gasification resulting in channeling through the carbon.

REFERENCES

1. Everett, M. R., Kinsey, D. V., and Romberg, E., *in* "Chemistry and Physics of Carbon" (P. L. Walker, Jr., Ed.), Vol. 3, p. 289. Marcel Dekker, New York, 1968.
2. McKee, D. W., *Carbon* **17,** 419 (1979).
3. McKee, D. W., and Yates, J. T., Jr., *J. Catal.* **71,** 308 (1981).

4. Otto, K., Bartosiewicz, L., and Shelef, M., *Carbon* **17,** 351 (1979).
5. Otto, K., and Shelef, M., *Carbon* **15,** 317 (1977).
6. Heintz, E. A., and Parker, W. E., *Carbon* **4,** 473 (1966).
7. Amariglio, H., Ph.D. Thesis, University of Nancy, France, 1962.
8. Baker, R. T. K., and Harris, P. S., *J. Sci. Instrum.* **5,** 795 (1970).
9. Baker, R. T. K., Sherwood, R. D., and Dumesic, J. A., *J. Catal.* **66,** 56 (1980).
10. Baker, R. T. K., and Sherwood, R. D., *J. Catal.* **70,** 198 (1981).
11. Baker, R. T. K., Sherwood, R. D., and Derouane, E. G., *J. Catal.* **75,** 382 (1982).
12. Baker, R. T. K., Feates, F. S., and Harris, P. S., *Carbon* **10,** 93 (1972).
13. Smith, C. S., "Grains, Phases and Interfaces: An Interpretation of Microstructure," Amer. Inst. Mining Met. Engrs., Inst. Metals. Div., Tech. Pub., No. 2387; *Metals Technol.* **15,** 37 pp. (June 1948).
14. Overbury, S. H., Bertrand, P. R., and Somorjai, G. A., *Chem. Rev.* **75,** 547 (1975).
15. Derouane, E. G., Baker, R. T. K., Dumesic, J. A., and Sherwood, R. D., *J. Catal.* **69,** 101 (1981).
16. Magne, P., and Duval, X., *Carbon* **11,** 475 (1973).
17. Holstein, W. L., and Boudart, M., *J. Catal.* **75,** 337 (1982).
18. Cairns, J. A., Keep, C. W., Bishop, H. E., and Terry, S., *J. Catal.* **46,** 120 (1977).
19. Thomas, J. M., *in* "Chemistry and Physics of Carbon" (P. L. Walker, Jr., Ed.), Vol. 1, p. 122. Marcel Dekker, New York, 1965.
20. Keep, C. W., Terry, S., and Waite, R. J., *in* "Gas Chemistry in Nuclear Reactors and Large Industrial Plant" (A. Dyer, Ed.), p. 196. Heyden, 1980.
21. McKee, D. W., *Fuel* **59,** 308 (1980).